Proceedings, Bicycle and Motorcycle Dynamics 2010
Symposium on the Dynamics and Control of Single Track Vehicles,
20–22 October 2010, Delft, The Netherlands

Some Investigations on the Wobble Mode of a Bicycle

Chr. Ott, B. Angrosch, J. Edelmann, M. Plöchl

Institute of Mechanics and Mechatronics
Vehicle System Dynamics and Biomechanics
Vienna University of Technology
Wiedner Hauptstraße 8-10, 1040 Vienna, Austria
e-mail: m.ploechl@tuwien.ac.at

ABSTRACT

Wheel shimmy and wobble are well known dynamic phenomena at automobiles, aeroplanes and motorcycles. This eigenmode excites in particular oscillations of the wheel about the steering axis, and it is no surprise, that unstable bicycle wobble is perceived unpleasant or may be dangerous, if not controlled by the rider in time.

Basic research on wobble at motorcycles within the last decades has revealed a better understanding of reasons for the sudden onset of wobble, and the complex relations between parameters affecting wobble have been identified. These fundamental findings have been transferred to bicycles. As mass balances and inertial properties, rider influence and lateral compliances of tyre and frame do differ at bicycle and motorcycle, approved models to represent wobble at motorcycles have to prove themselves, when applied at bicycles. For that purpose numeric results are compared with measurements at test runs, and parametric influences on the stability of the wobble mode at bicycles have been evolved. All numeric analysis and measurements are based on a specific test bicycle equipped with a steering angle sensor, wheel-speed sensor, GPS and a 3-axis accelerometer and angular velocity gyroscopic sensor.

Keywords: bicycle dynamics, wobble, shimmy, stability

1 INTRODUCTION

Learning how to ride a bicycle demands some courage. After some unfortunate experiences with a bicycle toppling over at low speeds, taking a risk to speed-up will be rewarded, as the bicycle may stabilize its motion on its own. Some more practice, and we have learnt how to handle two potentially unstable modes of the bicycle – weave and capsize.

There remains a further mode, wobble, which is – once experienced in its unstable form – at least unpleasant if not hazardous at all. Wobble is related to the more general class of wheel-shimmy, which is a self-excited motion of the wheel about the steering axis, and thoroughly treated in [1, 2]. The experience and main findings from detailed analysis of this phenomenon at motorcycles, e.g. [3], may hence be transferred to the bicycle. Although key issues on the wobble mode at bicycles are given in [4, 5], bicycle wobble is rarely addressed in scientific literature.

This paper aims to contribute to the analysis of the (low speed) wobble mode by examining a specific bicycle, that shows an unstable wobble mode at certain speeds, both on the basis of a mathematical model and by experiment. The considered bicycle is equipped with measurement devices (6 degree of freedom inertial measurement unit for accelerations and angular velocities, steering angle potentiometer, wheel-speed sensor, GPS).

Section 2 describes the mathematical system model used for the numerical analysis of stability, in Section 3 the test bicycle is introduced. Numerical results of influences on bicycle wobble are confronted with observations from test runs in Section 4, and finally, some Conclusions are drawn.

2 MATHEMATICAL SYSTEM MODEL

By examining a specific bicycle, both on the basis of a mathematical model and on test runs, influences on the wobble mode of a bicycle are to be found. For numerical analysis the real bicycle has to be represented by a mathematical system model of bicycle (and rider).

The Whipple or benchmark model, [6], can cover the capsize and weave mode. To account also for the wobble mode, the benchmark model is extended by lateral slipping tyres and frame compliance. Introducing a rotational degree of freedom φ_r for the upper torso of the rider results in the depicted system model, Figure 1. Besides the mass of the upper torso m_r, the model consists of the masses for the mainframe m_m, including the lower part of the rider and the rear wheel, front upper frame m_f and front subframe m_s, including the front wheel.

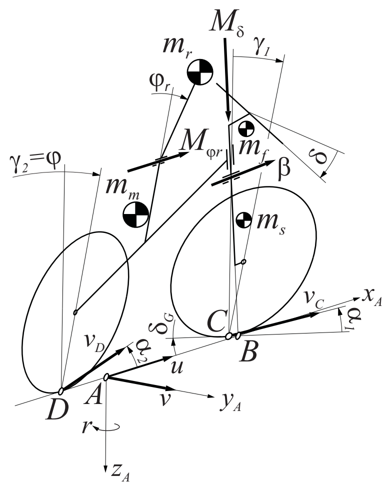

Figure 1. Bicycle model in cornering position.

The bicycle is shown while it moves at a roll angle φ of the mainframe and with a steering angle δ of the front fork about the steering axis, that is defined by a steering axis angle ε and a caster length t_c in upright position, see Figure 2. The rotational degree of freedom β at the steering head considers the frame compliance by a spring-damper element. The position of reference point A is at upright position of the bicycle below the centre of gravity of the mainframe and moves forward with constant longitudinal velocity u and velocity v in lateral direction, the intersection line $\overline{BD}$ rotates with yaw rate r. M_δ accounts for the applied steering torque at the handle bar, $M_{\varphi r}$ for the lean torque, and together they constitute the input vector to the system.

Although the nonlinear equations of motion are derived by applying a multibody formalism for the kinematics and d'Alembert's principle by hand, a subsequent linearization with respect to the upright, rectilinear motion results in the same linear equations of motion as presented in [2] for the motorcycle. The same nomenclature is used here. Mass properties and geometric data, required for the later numerical analysis, are obtained from data sheets of the test bicycle manufacturer or have been measured. The substitutive spring and damper values between upper torso and legs have been taken from literature, e.g. [7], other rider parameters from an anthropometric model, [8, 9].

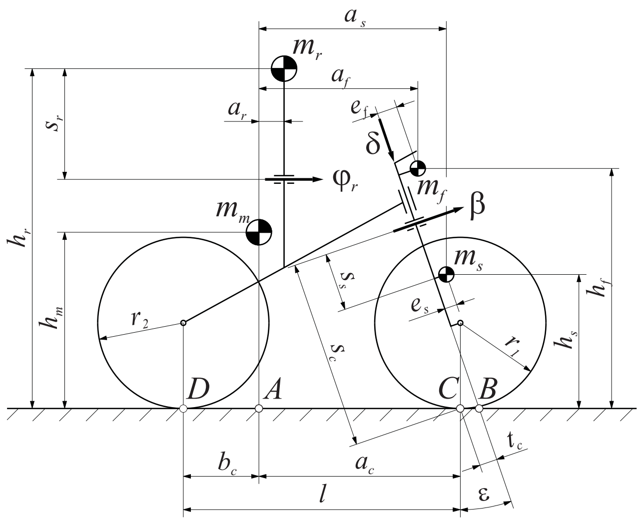

Figure 2. Bicycle model in upright position.

The spring characteristic, representing the elasticity at the steering head, has been measured on a test rig, but is later modified to match the measured wobble frequencies.

To determine the front and rear tyre forces and torques, the respective side slip angles $\alpha_{1,2}$,

$$\alpha_1 = \delta_G - \arctan\left(\frac{v_{C,y_A}}{v_{C,x_A}}\right), \quad \alpha_2 = -\arctan\left(\frac{v_{D,y_A}}{v_{D,x_A}}\right), \tag{1}$$

and camber angles $\gamma_{1,2}$ are required, with the ground steering angle δ_G and the corresponding components of the speed of propagation of the tyre contact centres C and D, with which these points move over the road surface. To account for dynamic properties of tyre force generation, a linear description to calculate transient side slip angles $\alpha'_{1,2}$ and camber angles $\gamma'_{1,2}$ is introduced,

$$\frac{\sigma_{\alpha i}}{u}\dot{\alpha}'_i + \alpha'_i = \alpha_i, \tag{2}$$

$$\frac{\sigma_{\gamma i}}{u}\dot{\gamma}'_i + \gamma'_i = \gamma_i, \qquad i = 1, 2\,. \tag{3}$$

Since the forward velocity u is chosen constant (with pure rolling in longitudinal direction) and aerodynamic drag is disregarded, the wheel loads F_{zi} are simply calculated from static equilibrium, neglecting the change of the position of the tyre contact point C due to steering and rolling. Finally, the lateral tyre forces F_{yi}, the self-aligning torques M_{zi} and the overturning couples M_{xi} are derived by, see Figure 3,

$$F_{yi} = c_{F\alpha i}\alpha'_i + c_{F\gamma_i}\gamma'_i\,, \tag{4}$$

$$M_{zi} = -c_{M\alpha i}\alpha'_i + c_{M\gamma_i}\gamma'_i\,, \tag{5}$$

$$M_{xi} = -c_{Mx\gamma i}\gamma_i\,. \tag{6}$$

The linear parameters of the tyre model have been estimated and adapted to results from test runs, [10, 11].

After derivation of the Jacobi matrices, d'Alembert's principle is applied to constitute the nonlinear set of system equations. Linearization with respect to the upright, rectilinear motion, with no roll or steering torque applied,

$$\dot{\underline{x}} = \mathbf{A}\underline{x} \quad \text{with} \quad \underline{x} = (\varphi, \varphi_r, \delta, \beta, v, r, \dot{\varphi}, \dot{\varphi}_r, \dot{\delta}, \dot{\beta}, \alpha'_1, \gamma'_1, \alpha'_2, \gamma'_2)^T \tag{7}$$

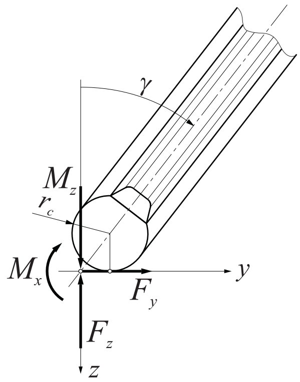

Figure 3. Forces and moments acting on bicycle tyre.

yields the system matrix $\mathbf{A}$. Eigenvalues λ_i of $\mathbf{A}$ need to be all negative for an asymptotic stable motion.

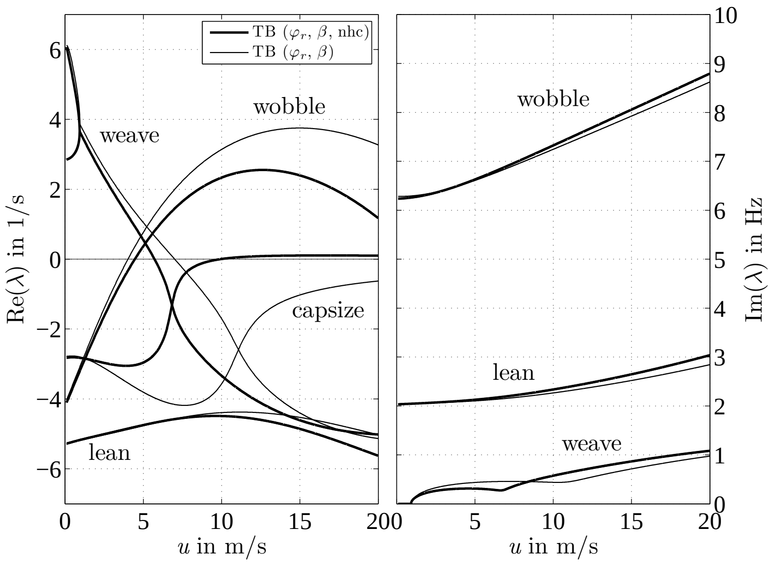

Figure 4. Test bicycle model (including the rider) with non-holonomic constraints in lateral direction at the contact points (thick line) and with lateral slipping tyres (thin line).

In the plot of Figure 4 the real and imaginary parts of corresponding eigenvalues can be compared for the test bicycle model with lateral slipping tyres (thin line) and for the test bicycle model with non-holonomic constraints in the lateral direction at the respective contact points instead (thick line). Only relevant modes are displayed in the figure. As a result, the considered tyre model "destabilizes" wobble and weave, and stabilizes capsize for all velocities.

Note the pronounced speed dependent increase of the wobble frequency between 6 and 9 Hz.

3 TEST BICYCLE AND MEASUREMENT EQUIPMENT

To compare numerical findings with observations from test runs, a commercially available trekking bicycle has been equipped with measurement devices, main data in Table 1. The test bicycle, Figure 5, shows a pronounced unstable wobble mode at certain speeds, where amplitudes of the steering oscillations increase quickly. Only low speed wobble is considered here.

Table 1. Main data of test bicycle and rider.

bicycle mass	14.5	kg
mass of measurement devices	3.5	kg
wheel size	28	inch
wheel base	1.095	m
steering head angle	71	^{o}
caster length	70.9	mm
fork offset	40	mm
rider mass	83	kg
rider size	1.83	m

A data logger, fixed to the rear rack, stores the measured sensor data on a flash card at rates up to 100 Hz. Also in the box is a 6 DOF inertial measurement unit, which provides 3-axis accelerations (maximum 10 g) and angular velocities (maximum 300 ^{o}/s), and a 20 Hz GPS-antenna. As it is difficult to transform the GPS measured velocity at the antenna to the fictive point A with sufficient accuracy due to the rolling and yawing motion, an additional wheel-speed sensor is applied at the rear frame. The sensor is based on the "hall effect" and the required metallic disc is made with 50 trigger holes.

An analog throttle angle sensor for motorcycles is used to measure the steering angle. The sensor is attached on a plate that is supported by lockable ball joints to the frame and plunged over a modified handle bar screw. In this way positional adjustment was rather easy.

Figure 5. Test bicycle used for measurements.

The tests have been performed on a straight bicycle path with small grade, which should help to keep a constant speed after stopping pedalling. Nevertheless, speed usually increased, often also due to tailwinds, see e.g. increase of speed between 16.5 and 20 s in Figure 6. After the rider has reached a designated speed, he stops pedalling and takes his hands off the handle bar in an upright position.

The focus of the test runs was to find out the wobble speed, which is defined here as the speed, when unstable wobble appears first with increasing speed, and frequencies of wobble oscillations.

It turned out, that it is quite a big challenge to come to the same wobble speed, when tests are repeated after some time. That's why the rider was instructed to tense his back muscles as strong as he can, in the upright position, to assure a firm connection with the saddle, and to initiate wobble by a lateral kick on the end of the handle bar, as a kind of defined initial disturbance. Otherwise it was by accident, if a disturbance appeared or not, that could force wobble, or the influence of the rider was unpredictable.

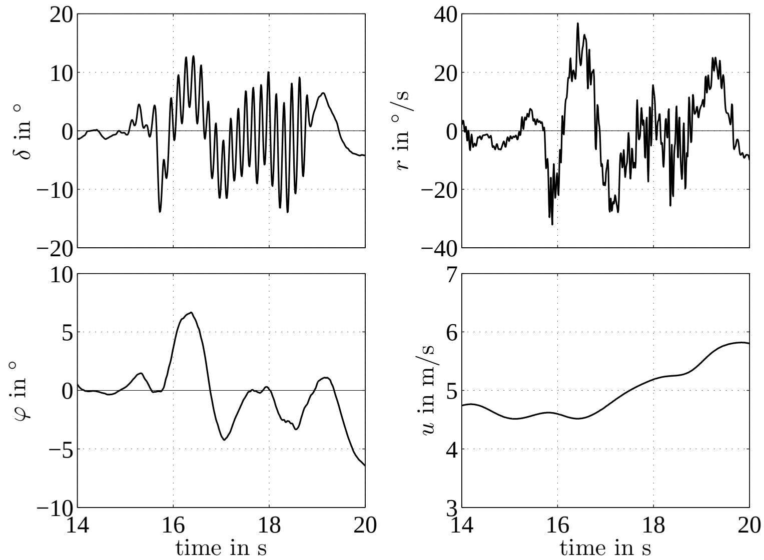

Figure 6. Example of measurements from a test run with wobble and weave.

Figure 6 shows as an example of a particular test run steering and roll angle, yaw rate and longitudinal speed. Between 15.5 and 18.5 s an increasing wobble oscillation superimposed by weave shows up. The wobble frequency can be identified with 6.4 Hz, the weave frequency with 0.65 Hz. At about 18.5 s, intervention of the rider was required to break the wobble oscillation for a save ride.

4 DISCUSSION OF RESULTS

The following subsections shall reveal main influences of the tyre, rider, front steering assembly and frame, exclusively on the bicycle wobble mode.

4.1 Tyre influence on wobble

With respect to the tyre properties, the most significant parameter affecting wobble, and the corresponding wobble frequency, is the cornering stiffness of the front tyre. For sake of clearness the shown parameter variations are exaggerated, Figure 7. The thick line represents the standard configuration (test bicycle, TB). At the thin line the respective parameter is only half its value, at the dotted line double. Large cornering stiffness at the front tyre reveals a "destabilizing" effect and higher frequencies. The camber stiffness does not affect wobble, but weave. For the standard configuration the wobble speed is about 14 km/h (4 m/s).

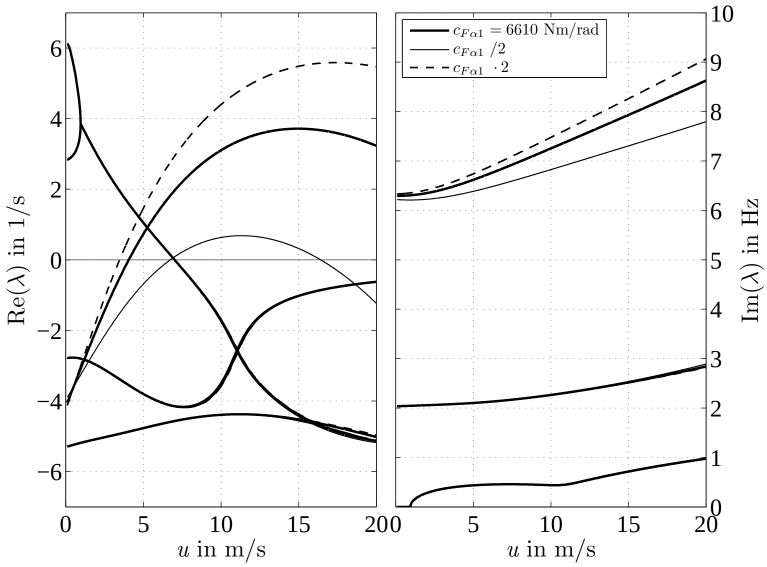

Figure 7. Variation of cornering stiffness of the front tyre, 4 bar.

A small "destabilizing" effect can be noticed for increasing relaxation length for the front side slip angle, [11]. Both parameters, cornering stiffness and relaxation length, are related to the inflation pressure and contribute adversely on the wobble speed. However, test runs suggest a small "destabilizing" effect at increased inflation pressure, 6 bar. The little influence of pressure change, at least for the considered tyre and bicycle, is affirmed by only small changes of measured wobble frequencies.

In Figure 8 data points (real and imaginary parts) from measurements (wobble oscillations) have been (approximated and) included. They are derived from test runs with three, quite different types of treads. The left tyre belongs to the standard configuration, and is a worn tyre. From the measured wobble frequencies, which fit quite well to the numerical results, may be concluded, that cornering stiffness may decrease from the left to the right tyre, although differences are rather small. Also the differences in wobble speed are rather marginal. Anyway, the plot gives some evidence that chosen parameters map the real bicycle behaviour very reasonable.

Increasing the spin moment of inertia of the front tyre moves the wobble and weave mode in the direction of the stable area, but cannot eliminate wobble of the specific test bicycle at all. This has been confirmed by test runs with a similar amount of increase of the wobble speed and decrease of the corresponding frequency, [11].

4.2 Rider influence on wobble

In general, a soft grip of the handle bar by the rider may help to avoid wobble. But also at hands off test runs, the rider is important with respect to wobble.

If the rider is very light, wobble may even not be present at all, but at least the wobble speed is moved to higher speeds. All modes are strongly influenced by the mass properties of the rider, as can be observed both in Figure 9 and at test runs. For the light rider the wobble speed is increased

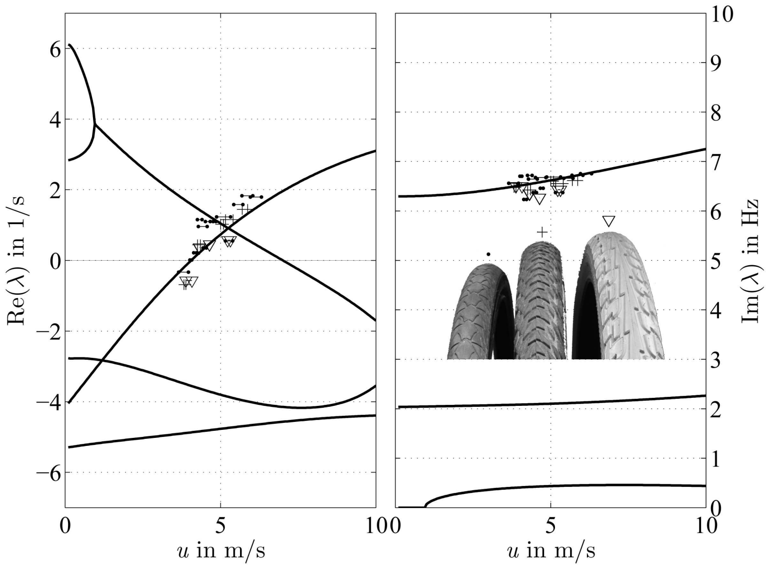

Figure 8. Comparison of numerical results with measured data.

from about 14 km/h to about 20 km/h (5.6 m/s), also to be noticed by the triangle-marks close to the real axis. The wobble frequency is about 0.5 Hz higher.

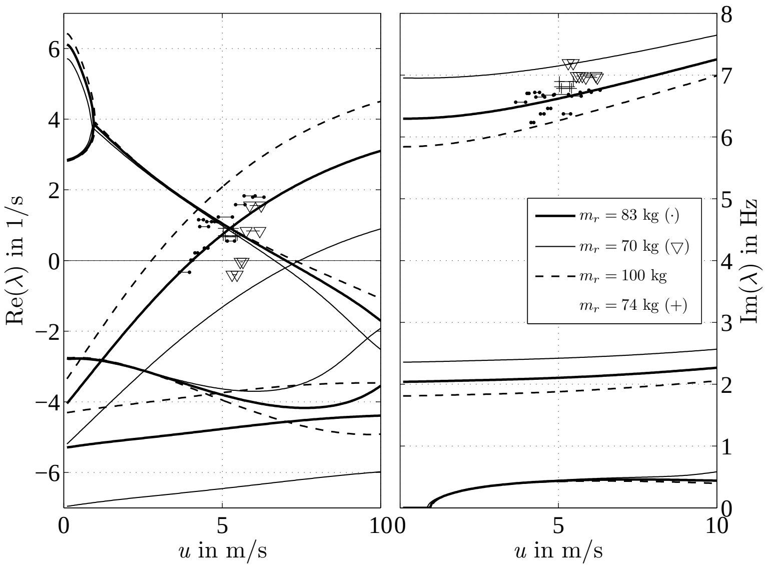

Figure 9. Variation of rider mass.

Although the position of the rider does show some influence on wobble, the wobble speed is affected only marginally. Loading the front tyre and increasing thus the cornering stiffness is usually disadvantageous with respect to wobble.

The hinge above the hip allows for a rotation of the upper body about the longitudinal axis and is suspended by a respective spring-damper element. The lower extremities are considered to be fixed to the main frame, while a rotational, passive motion of the upper body is assumed only. In Figure 10 the corresponding spring stiffness is changed from "loose" to "tense". Almost no influence on weave and wobble can be noticed, however, the lean mode is affected considerably without surprise.

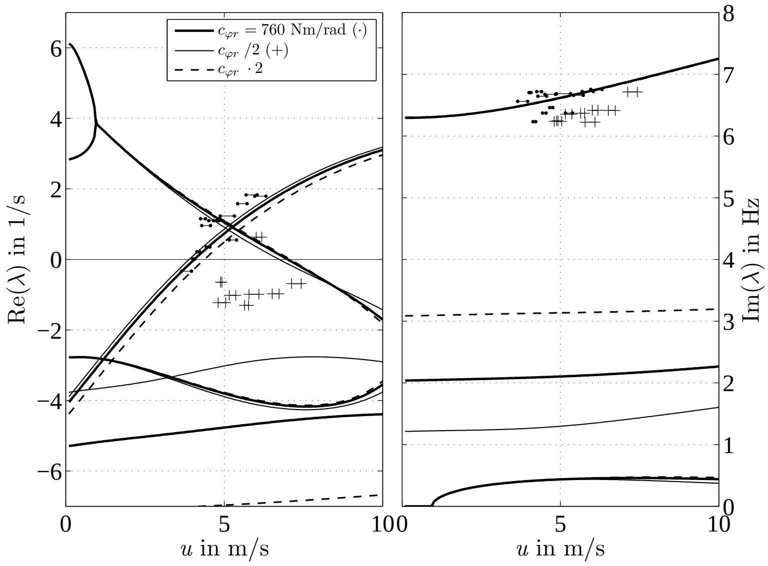

Figure 10. Variation of hip stiffness of rider.

The "doted" data points in the plot correspond to the standard test instructions, full tension of back muscles, while the "plus" marks to a relaxed upright position of the rider. The wobble frequencies corresponding to the relaxed position are somewhat smaller than for the tight position. The "plus" marks in the left plot indicate a negative real part of the respective eigenvalues, and thus reveal a stable wobble mode, observed in the test runs. In a relaxed position is was almost impossible to run into an unstable wobble mode at lower speeds. Therefor is no agreement with the derived wobble mode with the soft spring, which consequently cannot map a relaxed position of the rider at all! For a correct representation of the damped wobble mode at relaxed position, an energy absorbing element may be added to model the lateral firmness of the contact of the rider at the saddle. Obviously, a firm contact with the saddle by pressing legs together supports the onset of wobble and sustains wobble, while unloading the saddle may restrain wobble.

4.3 Influence of steering assembly on wobble

Increasing the steering axis angle ε at constant fork offset $(r_1 \sin\varepsilon - t_c)$ and wheel base l results in a more flat steering axis and adjunctive longer mechanical trail, and reveals some "stabilizing" effects. However, consequent implications on the tyre (model) maintain an unstable wobble mode, [11]. The corresponding wobble frequencies increase considerably, while weave frequencies are somewhat smaller at higher speeds.

Putting some extra load in the front or rear rack moves all modes (wobble in the direction of the unstable area), and results in smaller wobble frequencies. A distinct wobble mode due to the extra load in the front rack is mainly a consequence of the added mass (high) to the steering assembly, exciting roll and consecutive steering oscillations. All other effects due to the added mass contribute less (or adversely, like the increased moment of inertia with respect to the steering axis). The numeric analysis in [11] confirm the assumptions on wobble in [5]. The mass distribution of the steering assembly is in particular important with respect to the wobble mode. However, the complex relations demand a quantitative evaluation to find out about contradictious effects.

4.4 Frame influence on wobble

Although tyre properties, mass balance and geometric properties of the front assembly can be used to tune the wobble mode of the considered test bicycle to some extent, the frame compliance contributes most, Figure 11. The substitutive stiffness between main frame and front assembly affects the wobble frequency considerably, but only marginally weave and capsize. It is not the substitutive lateral stiffness, but to a large extent related damping that may stabilize or "reduce" wobble.

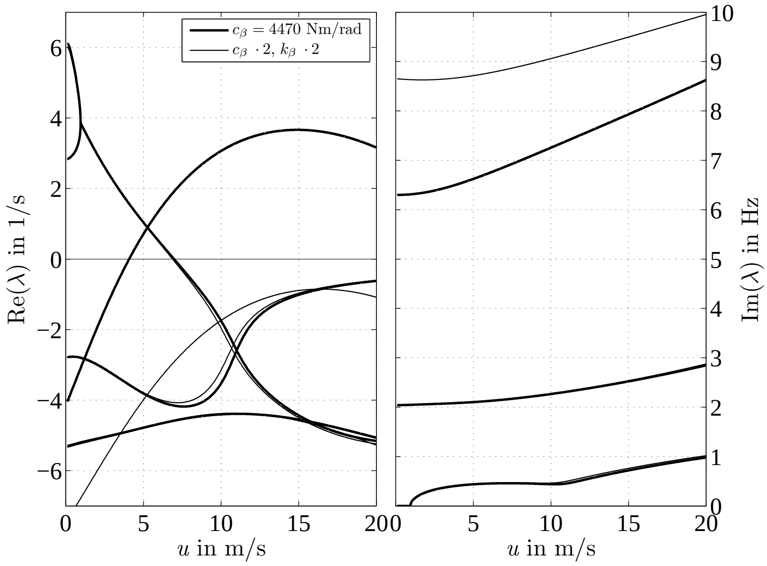

Figure 11. Variation of substitutive stiffness and damping at the steering head.

The section modulus of the diagonal tube of the analyzed test bicycle with respect to lateral bending is much smaller compared to vertical bending. Also the geometric connection properties to the steering tube seem rather soft. These inverted effects may be the reason for the extensive wobble of the test bicycle.

5 CONCLUSIONS

Wobble can be excited with hands on and off the handle bar, and is unpleasant, if not hazardous at all. The rider may influence the onset of wobble, and be able to break down wobble when occurring, at least at low speeds.

Test runs and accompanied measurements have revealed that mathematical models and numeric analysis are able to support a proper design of the dynamical behaviour of bicycles accounting for aspects of stability, handling and comfort. In this way, some responsibility is moved from the rider to the manufacturer.

The applied mathematical system model has approved to be qualified to identify design parameters and effects that promote unstable wobble. However, the model may be improved by incorporating the firmness of the rider's connection to the saddle, and detailed consequences for the design of the frame with respect to the substitutive steering head stiffness and damping, introduced in the bicycle model, need yet to be addressed.

REFERENCES

[1] I. J. M. Besselink, ”Shimmy of aircraft main landing gears”, Dissertation, TU-Delft, 2000.

[2] H. B. Pacejka, *Tyre and Vehicle Dynamics*, Butterworth and Heinemann, Oxford, 2002.

[3] R. S. Sharp, C. J. Alstead, ”The influence of structural flexibilities on the straight running stability of motorcycles”, *Vehicle System Dynamics* **9** (1980), pp. 327-357.

[4] R. S. Sharp, D. J. N. Limebeer, ”Bicycles, motorcycles, and models”, *IEEE Control Systems Magazine* (2006), pp. 34-61.

[5] R. S. Sharp, ”On the stability and control of the bicycle”, *Applied Mechanics Reviews*, *61* (2008).

[6] J. P. Meijaard, J. M. Papadopoulos, A. Ruina, A. L. Schwab, ”Linearized dynamics equations for the balance and steer of a bicycle: a benchmark and review”, *Proceedings of the Royal Society A* (2007), pp. 1955-1982.

[7] R. S. Sharp, D. J. N. Limebeer, ”On steering wobble oscillations of motorcycles”, *Proceedings Instn Mech Engrs Vol. 218 Part C: J. Mechanical Engineering Science* (2004), pp. 1449-1456.

[8] NASA Main System Integration Standards Volume I, Section 3 Anthropometry and Biomechanics, http://msis.jsc.nasa.gov/sections/ section03.htm, Stand vom 1. Dezember 2009.

[9] E. P. Hanavan, JR. Captain, *USAF A mathematical model of the human body*, AMRL-TR-64-102, AD-608-463, Aerospace Medical Research Laboratories, Wright Patterson Air Force Base/Ohio, 1964.

[10] B. Angrosch, ”Fahrradstabilität unter besonderer Berücksichtigung des Lenkungsflatterns”, Diploma-Thesis, Vienna University of Technology, 2010.

[11] Chr. Ott, Diploma-Thesis, to be submitted in 2010, Vienna University of Technology.